



Published in final edited form as:

*Kidney Int.* 2016 September ; 90(3): 568–579. doi:10.1016/j.kint.2016.04.025.

## Insulin and the PI3K/AKT Signaling Pathway Regulate Ribonuclease 7 Expression in the Human Urinary Tract

Tad Eichler<sup>1</sup>, Brian Becknell<sup>1,2</sup>, Robert S. Easterling<sup>1,3</sup>, Susan E. Ingraham<sup>1,2</sup>, Daniel M. Cohen<sup>4</sup>, Andrew Schwaderer<sup>1,2</sup>, David S. Hains<sup>5</sup>, Birong Li<sup>1</sup>, Ariel Cohen<sup>1</sup>, Jackie Metheny<sup>1</sup>, Susheela Trindandapani<sup>6</sup>, and John David Spencer<sup>1,2,\*</sup>

<sup>1</sup>Center for Clinical and Translational Research, The Research Institute at Nationwide Children's, Columbus, OH, USA

<sup>2</sup>Division of Nephrology, Department of Pediatrics, Nationwide Children's, Columbus, OH, USA

<sup>3</sup>University of Toledo College of Medicine and Life Sciences, Toledo, OH, USA

<sup>4</sup>Division of Emergency Medicine, Department of Pediatrics, Nationwide Children's, Columbus, OH, USA

<sup>5</sup>Innate Immunity Translational Research Center, Children's Foundation Research Institute at Le Bonheur Children's Hospital, Memphis, TN, USA

<sup>6</sup>Comprehensive Cancer Center, Department of Internal Medicine and Department of Molecular Virology, Immunology, and Medical Genetics, The Ohio State University James Cancer Hospital and Richard J. Solove Research Institute, Columbus, OH, USA

### Abstract

Diabetes mellitus is a systemic disease associated with a deficiency of insulin production or action. Diabetic patients have an increased susceptibility to infection with the urinary tract being the most common site of infection. Recent studies suggest that Ribonuclease 7 (RNase 7) is a potent antimicrobial peptide that plays an important role in protecting the urinary tract from bacterial insult. The impact of diabetes on RNase 7 expression and function are unknown. Here, we investigate the effects of insulin on RNase 7. Using human urine specimens, we measured urinary RNase 7 concentrations in healthy control patients and insulin-deficient type 1 diabetics before and after starting insulin therapy. Compared to controls, diabetic patients had suppressed urinary RNase 7 concentrations, which increased with insulin. Using primary human urothelial cells, we explored the mechanisms by which insulin induces RNase 7. Insulin induces RNase 7 production via the phosphatidylinositol 3-kinase signaling pathway (PI3K/AKT) to shield urothelial cells from uropathogenic *E. coli*. In contrast, we show that uropathogenic *E. coli* suppresses PI3K/AKT and RNase 7. Together, these results indicate that insulin and PI3K/AKT signaling are essential for RNase 7 expression. They also suggest that increased infection risks in diabetic patients may be

\*Address correspondence to: John David Spencer, Center for Clinical and Translational Research, The Research Institute at Nationwide Children's, 700 Children's Drive, Columbus, Ohio 43205 USA, Phone: 614-722-4371, Fax: 614-722-6482, John.Spencer@nationwidechildrens.org.

#### Disclosure and Competing Interests

The authors have no conflicts of interest or relevant financial relationships related to this manuscript to disclose.

secondary to suppressed RNase 7 production. These data may provide unique insight into novel UTI therapeutic strategies in at risk populations.

## Keywords

pyelonephritis; diabetes; urology; cell signaling

## Introduction

Diabetes mellitus (DM) is associated with many complications, including increased infection risk. With diabetes, the most common site of bacterial infection is the urinary tract.<sup>1</sup> Urinary tract infection (UTI) is ten times more common in patients with DM. In diabetic patients, UTI is more likely to cause acute kidney injury and renal scarring, which increase the risk of chronic kidney disease.<sup>2-4</sup> Complicated UTIs, including emphysematous pyelonephritis, renal abscess, and necrotizing papillitis are also more common.<sup>5, 6</sup> The risk of bacteremia is four times greater in diabetic patients with UTI than non-diabetic patients. Moreover, mortality rates are nearly five-fold greater.<sup>7, 8</sup> In 2011, estimated costs for UTI management in diabetic patients exceeded three billion dollars.<sup>1</sup> Currently, no treatment strategy has proven effective for UTI prevention in DM patients. In part, this stems from an incomplete understanding of how DM impacts urinary tract host defense mechanisms.

Recent evidence suggests that antimicrobial peptides (AMP) shield urinary tract from invading pathogens. AMPs, which serve as natural antibiotics, are an essential component of the innate immune system and have the potential to be developed as novel UTI therapeutics.<sup>9-11</sup> Our research group has identified Ribonuclease 7 (RNase 7) as a potent, front-line human AMP that is produced by the urothelium of the bladder and renal intercalated cells.<sup>12, 13</sup> RNase 7 is one of the most abundant AMPs in human urine. It rapidly kills Gram-positive and Gram-negative uropathogens at micromolar concentrations.<sup>12, 14</sup> RNase 7's bactericidal properties are independent of its catalytic activity and are dependent on its ability to disrupt the microbial cell wall.<sup>13, 15-18</sup> RNase 7 has been described as the most potent human AMP.<sup>13, 19, 20</sup> When it is neutralized in human urine specimens, urinary bacterial growth increases – suggesting that deficient urinary RNase 7 production increases UTI susceptibility.<sup>12, 21</sup>

Because patients with DM have an increased propensity to develop UTI, we hypothesized that they have suppressed RNase 7 production – rendering them more susceptible to infection. Additionally, because DM is associated with insufficient insulin production and/or action, we hypothesized that insulin regulates RNase 7 production. Here, we investigate RNase 7 expression in patients with type 1 diabetes mellitus (T1DM). In doing so, we evaluate the effects of insulin on RNase 7 production. Because the phosphatidylinositide 3-kinase (PI3K/AKT) pathway is a key regulator of insulin signaling, we also investigate how PI3K/AKT activity regulates RNase 7 production. PI3K/AKT signaling is activated when insulin binds to its receptor (Figure 1).<sup>22-25</sup>

## Results

### Diabetic patients have low urinary RNase 7 concentrations that increase with insulin therapy

To investigate if insulin deficiency alters RNase 7 expression, we quantitated urinary RNase 7 concentrations in healthy control children ( $n=30$ ) and compared them to urinary RNase 7 concentrations from children presenting to the Emergency Department with new-onset T1DM ( $n=30$ ).

Urine specimens and laboratory studies from the T1DM children were collected before insulin therapy was initiated (Supplemental Table 1). ELISA results demonstrate that children with new-onset T1DM had significantly lower median urinary RNase 7 concentrations, normalized to urine creatinine (UCr) (median: 0.87  $\mu\text{g}/\text{mg}$  UCr, range: 0.017–2.79  $\mu\text{g}/\text{mg}$  UCr), than control children (median: 1.79  $\mu\text{g}/\text{mg}$  UCr, range: 0.28–3.46  $\mu\text{g}/\text{mg}$  UCr,  $p=0.0002$ , Figure 2A).

In the new-onset T1DM patient cohort, serum insulin levels were measured in 19/30 children at presentation as part of clinical care. In these 19 children, we observed a moderate positive correlation between urinary RNase 7 concentrations and serum insulin levels ( $r^2=0.27$ ;  $p=0.023$ , Figure 2B). In contrast, we did not observe a correlation between urinary RNase 7 concentrations and the estimated glomerular filtration rate, initial hemoglobin A1c (HbA1c), serum glucose, or urine glucose (Supplemental Figure 1).

To further investigate whether systemic insulin therapy regulates urinary RNase 7 concentrations, follow-up urine specimens were collected from new-onset T1DM patients at least 30 days after starting insulin ( $n=30$ ). ELISA results show that median urinary RNase 7 concentrations increased to 1.25  $\mu\text{g}/\text{mg}$  UCr (range: 0.43–5.32  $\mu\text{g}/\text{mg}$  UCr) after starting insulin therapy ( $p=0.0024$ , Figure 2A). These urinary concentrations were not significantly different than the median urinary RNase 7 concentration in the control group ( $p=0.167$ ). When assessed on an individual basis, urinary RNase 7 concentrations increased in 80% of patients (range of fold increase: 0.3–12.56, Supplemental Figure 2). At the 30-day follow-up evaluation, serum insulin levels were not collected as part of clinical care. Together, these results suggest that insulin induces urinary RNase 7 expression.

### The bladder urothelium and renal intercalated cells express insulin receptor and RNase 7

Previously, we have demonstrated that the bladder urothelium and the intercalated cells of the renal collecting tubules produce RNase 7.<sup>12, 26</sup> Prior evidence also suggests that the insulin receptor (IR) is expressed throughout the nephron and collecting tubules.<sup>27</sup> However, there is limited evidence evaluating IR expression in the human kidney and urinary tract.<sup>28–30</sup> To investigate the relative localization of RNase 7 to IR, we performed immunostaining on human tissues. Immunohistochemistry (IHC) demonstrates that IR and RNase 7 are produced by the urothelium of the bladder. Negative controls demonstrated no IR or RNase 7 expression (Figure 3).

Immunofluorescence (IF) allowed us to localize IR and RNase 7 production in the renal collecting tubules. Triple labeling IF shows that the intercalated cells of the collecting

tubules, identified by positive anion exchanger- 1 (AE-1) or V-ATPase staining, co-express IR and RNase 7 (Figure 4 and Supplemental Figure 3). This co-localized and cell-specific expression of IR and RNase 7 in the bladder urothelium and renal intercalated cells offers insight into the relationship between insulin signaling and RNase 7 production.

### Insulin induces RNASE7 mRNA expression in vitro

To further evaluate the effects of insulin on RNase 7 expression, we cultured primary human urothelial cells (HUC) and primary human renal epithelial cells (HRC) in insulin-free media and treated them with recombinant human insulin. Quantitative real-time PCR shows that insulin induced *RNASE7* gene expression over time (Figure 5). Insulin also induced mRNA expression of several other genes in the Ribonuclease A Superfamily (Supplemental Figure 4).

### Insulin induces RNase 7 peptide production via PI3K/AKT

Because insulin is a known PI3K/AKT agonist, we hypothesized that insulin induces RNase 7 production via the PI3K/AKT pathway. In the HUCs and HRCs, Western blot confirmed that insulin induces AKT (ser473) phosphorylation over time (Figure 6). In the HUCs, Western blot also demonstrates that insulin induces RNase 7 peptide production over time and in a dose-dependent manner (Figure 6 and Supplemental Figure 5). These results were quantitated via densitometry (Supplemental Figure 6). RNase 7 was not routinely detected by Western blot in the HRCs (Figure 6). In both the HUCs and HRCs, we measured RNase 7 secretion into culture media via ELISA. In the HUCs, RNase 7 concentrations increased nearly two-fold (144.1±22.01 ng/mL to 305.4±32.68 ng/mL,  $p=0.009$ ) after twenty-four hours of insulin treatment (Figure 6B). Similarly, in the HRCs, insulin increased RNase 7 concentrations 2.7-fold twenty-four hours after treatment (38.09±5.24 ng/mL to 102.2±1.91 ng/mL,  $p=0.002$ , Figure 6D). Moreover, insulin induced RNase 7 secretion in a dose-dependent manner (Supplemental Figure 5).

To confirm that insulin-induced RNase 7 production is regulated by PI3K/AKT, cells were pretreated wortmannin, a covalent PI3K inhibitor. In the HUCs, Western blot shows that wortmannin pretreatment blocked insulin-induced AKT activation and downstream RNase 7 production (Figure 6). In both the HUCs and HRCs, ELISA demonstrates that wortmannin blocked RNase 7 secretion into the culture media (Figure 6). Similar results were observed with LY294002 pretreatment, a synthetic PI3K/AKT inhibitor (not shown). These results verify that insulin induces urothelial RNase 7 expression through the PI3K/AKT signaling cascade.

In support of these data, we blocked basal PI3K/AKT activity in *ex vivo* human kidney specimens ( $n=3$ ) with wortmannin and AKT Inhibitor X – a reversible and selective AKT inhibitor.<sup>31</sup> Western blot demonstrates that both wortmannin and AKT Inhibitor X suppressed renal PI3K/AKT activity and RNase 7 production. Similarly, ELISA assays demonstrate that PI3K/AKT inhibition decreased RNase 7 secretion (Supplemental Figure 7).

### AKT regulates urothelial RNase 7 expression

To further confirm that PI3K/AKT regulates urothelial RNase 7 expression, we transiently transfected 5637 bladder cells with (A) wild-type AKT (wt-AKT); (B) the constitutively active membrane targeted-PKB $\alpha$  (m/p-AKT); and (C) the dominant negative PKB $\alpha$ -K170A/T308A/S473A (DN-AKT). The m/p-AKT mutant contains a myristoylation signal that causes AKT translocation to the plasma membrane resulting in AKT hyperactivation.<sup>32, 33</sup> The DN-AKT mutant, which contains the mutations K179A (substitution of alanine for lysine at position 179), T308A (substitution of alanine for threonine at position 308), and S473A (substitution of alanine for serine at position 473), is a kinase-inactive, phosphorylation-deficient PKB $\alpha$ /AKT1 construct.<sup>34</sup> Western blot demonstrates that urothelial cells transfected with m/p-AKT had substantially elevated levels of AKT (ser473) phosphorylation while DN-AKT transfected cells had suppressed AKT (ser473) phosphorylation (Figure 7A).

Next, we used quantitative RT-PCR to evaluate *RNASE7* mRNA expression in transfected 5637 cells. We also measured RNase 7 peptide secretion into the urothelial cell culture media via ELISA. Our results demonstrate that *RNASE7* mRNA expression was significantly greater in m/p-AKT transfected cells compared to wt-AKT transfected cells ( $p=0.009$ , Figure 7B). Similarly, RNase 7 peptide concentrations in the culture media were significantly greater in m/p-AKT transfected cells compared to cells transfected with wt-AKT ( $p=0.029$ , Figure 7C). In contrast, cells transfected with DN-AKT had decreased *RNASE7* expression ( $p=0.021$ , Figure 7B) and suppressed basal release of RNase 7 into the culture media ( $p=0.019$ , Figure 7C). There were no significant differences in RNase 7 mRNA or peptide expression between cells transfected with wt-AKT and cells transfected with an irrelevant protein fused to mCherry (not shown).

### Insulin-induced RNase 7 production shields urothelial cells from UPEC

To evaluate if insulin-induced RNase 7 production suppresses UPEC growth, we isolated culture media from non-treated, insulin-treated, and wortmannin plus insulin treated HRCs and inoculated them with UPEC (strain CFT073). UPEC growth was assessed over time. UPEC growth was suppressed in the insulin-treated media samples – linking insulin and PI3K/AKT activity to UPEC growth suppression (Figure 8A, dashed line). In culture media isolated from wortmannin pretreated (diamond studded line) and wortmannin treated cells (black circles), UPEC growth increased – providing further evidence that PI3K/AKT activity is necessary to suppress UPEC growth. The addition of RNase 7 neutralizing antibody to insulin-treated cell media increased UPEC growth (solid black line), thereby linking UPEC growth suppression to RNase 7's antimicrobial activity. The addition of an irrelevant antibody had no effect on UPEC growth (not shown).

To confirm that insulin-induced RNase 7 production contributes to UPEC killing, we performed colony count assays in culture media isolated from non-treated, insulin-treated, and wortmannin plus insulin treated HRCs. Similar to the above results, UPEC (strain CFT073) killing increased in the insulin-treated media samples (Figure 8B). The application of RNase 7 neutralizing antibody significantly blocked the UPEC-killing activity of RNase 7. Similarly, wortmannin pretreatment diminished insulin-induced antimicrobial activity

(Figure 8B). Antimicrobial activity was not inhibited with the addition of an irrelevant antibody (not shown).

Next, to assess if insulin-induced RNase 7 production protects urothelial cells from UPEC insult, we challenged HRCs with UPEC (strain CFT073) and evaluated cellular cytotoxicity via lactate dehydrogenase (LDH) release into the culture media. LDH is a stable cytoplasmic enzyme that is present in most cells. It is released into the cell culture supernatant upon damage of the cytoplasmic membrane.<sup>35</sup> Five hours after UPEC challenge, LDH concentrations increased in the culture media (Figure 7C). LDH release was suppressed when cells were treated with insulin 24 hours prior to UPEC challenge. This effect was significantly diminished in the presence of RNase 7 neutralizing antibodies. Similarly, wortmannin pretreatment mitigated the protective effects of insulin, significantly increasing LDH release despite the presence of insulin (Figure 7C). Wortmannin or RNase 7 neutralizing antibody pretreatment did not affect basal cellular LDH release (not shown). These results suggest that RNase 7 contributes to cellular defense by killing UPEC and shielding urothelial cells from bacterial challenge. Moreover, they identify insulin and the PI3K/AKT signaling cascade as important mediators of host defense.

### UPEC inhibits urothelial PI3K/AKT activity and RNase 7 production

To evaluate UPEC's direct impact on RNase 7 production, we challenged bladder cells with UPEC. In this experiment, we used 5637 urothelial cells because they, like most transformed cells, have greater endogenous PI3K/AKT activity.<sup>36</sup> Prior evidence demonstrates that UPEC strains expressing  $\alpha$ -hemolysin (HlyA) inhibit PI3K/AKT activation in these cells.<sup>37</sup> Consistent with these studies, Western blot demonstrates that the HlyA producing UPEC strain UTI89 dephosphorylates AKT (Figure 8). Similar results were observed when 5637 cells were stimulated with the HlyA producing UPEC strain CFT073 or purified  $\alpha$ -hemolysin (Supplemental Figure 8). In contrast, targeted disruption of the *hlyA* gene in UTI89 (UTI89 *hlyA*), prevented AKT dephosphorylation (Figure 8). During these experiments, UPEC and  $\alpha$ -hemolysin did not compromise host cell integrity as assessed by trypan blue exclusion assays.

To investigate the effects of UPEC on RNase 7 expression, we probed the same immunoblots with anti-RNase 7 antibodies. Western blot demonstrates that HlyA producing UPEC strains and purified  $\alpha$ -toxin suppress RNase 7 expression at the same time points in which AKT is dephosphorylated (Figure 8 and Supplemental Figure 8). In contrast, UTI89 *hlyA*, which does not produce HlyA or inactivate AKT, had no effect on RNase 7 production. These results were quantitated via densitometry (Supplemental Figure 9). Overall, these results suggest that *E. coli* suppresses RNase 7 production by inactivating PI3K/AKT. Moreover, they specifically identify HlyA as a virulence factor that suppresses RNase 7.

### Discussion

In this study, we identify insulin as an important hormone that contributes to host defense by regulating RNase 7 production. Using human clinical samples, we show that urinary RNase 7 concentrations are suppressed in patients with insulin deficient, new-onset T1DM and that

urinary RNase 7 concentrations increase with insulin therapy. To support these data, we used primary human urothelial cell culture models to demonstrate that insulin induces RNase 7 production via the PI3K/AKT signaling pathway to suppress UPEC growth and shield urothelial cells. Finally, we show the HlyA producing UPEC strains can suppress PI3K/AKT activity and downstream RNase 7 production. Together, these results identify unique mechanisms that may explain why certain patient populations, like patients with DM, have increased UTI risk.

To our knowledge, this is the first report to demonstrate that RNase 7 expression is suppressed in diabetic patients. This is also the first study to suggest that insulin induces RNase 7 (and other RNase A Superfamily members). In support of these findings, prior studies suggest that T1DM patients have lower serum AMP concentrations of cathelicidin and human  $\beta$ -defensin 1 (hBD-1).<sup>38</sup> Prior studies also show that insulin increases AMP expression. Wang and colleagues found that insulin induces hepatic hepcidin production *in vitro* and *in vivo* through STAT3.<sup>39</sup> Using human embryonic kidney cells (HEK-293), Branea *et al* demonstrate that glucose plus insulin enhance hBD-1 mRNA expression. Quercetin, a PI3K/AKT and Protein Kinase C inhibitor, abrogated this effect.<sup>40</sup> Similarly, other groups have shown that insulin deficient diabetic rats have suppressed renal rat  $\beta$ -defensin 1 (rBD-1) gene expression compared to non-diabetic controls.<sup>41, 42</sup> Using streptozotocin-treated diabetic rats, Froy *et al* demonstrate that reduced rBD-1 mRNA and urinary rBD-1 peptide expression are restored with insulin.<sup>41</sup> These prior studies, coupled with our *in vitro* data and human urinary RNase 7 ELISA results, suggest that insulin may contribute to urinary tract sterility by boosting AMP production. Thus, identifying avenues to increase endogenous AMP production may decrease UTI risk and facilitate the development of novel AMP-based therapies. Given RNase 7's potent broad-spectrum antimicrobial activity, high urinary concentrations, abundant expression in other organs like the skin (which is a common site of infection in DM patients), and limited cytotoxicity toward urothelial cells and keratinocytes, we believe it is an ideal candidate to evaluate as a unique therapeutic for DM patients.<sup>10, 13, 43</sup>

In contrast to these findings, which were obtained using insulin deficient and/or T1DM models, Page *et al* used an experimental model of type 2 diabetes (T2DM) and found that rBD-1 mRNA expression was elevated in diabetic GK rat kidneys. rBD-1 expression correlated with high concentrations of biglycan and TGF- $\beta$ 1 – two markers of developing diabetic nephropathy.<sup>44</sup> This same research group also demonstrated that prolonged hyperglycemia increased hBD-1 mRNA and peptide expression in HEK-293 cells.<sup>45</sup> In our study, human urinary RNase 7 concentrations did not correlate with serum or urinary glucose concentrations. However, because the patients in our cohort presented to the Emergency Department with the acute onset of T1DM, they were less likely to have longstanding hyperglycemia or the side effects associated with chronic DM. Additional studies are ongoing to evaluate the effects of both T1DM and T2DM on RNase 7 expression, the impact of chronic hyperglycemia and poor glycemic control on AMP production, and the role of diabetic nephropathy on UTI risk.

In this study, we also demonstrate that insulin induces RNase 7 via PI3K/AKT. DM impacts PI3K/AKT signaling, and some reports suggest that patients with DM have reduced

PI3K/AKT activity.<sup>46</sup> The PI3K/AKT pathway is required for a diverse array of cellular activities. Over the last decade, PI3K/AKT signaling has become a focal point in arenas like oncology, neurologic disorders, and DM. More recently, PI3K/AKT activity has been recognized to impact microbial pathogenesis and host defense.<sup>47–49</sup> Previous evidence indicates that PI3K/AKT regulates RNase 3/Eosinophil Cationic Peptide and murine eosinophil associated RNase (mEAR) degranulation and secretion from human and murine granulocytes.<sup>50</sup> PI3K/AKT inhibition alters host inflammatory and innate immune responses, increases infection risk in different organ systems, and decreases survival.<sup>48, 49, 51–53</sup> Wortmannin inhibition of PI3K/AKT increases morbidity and mortality following experimental endotoxemia and polymicrobial sepsis.<sup>48, 49</sup> Clinically, patients receiving treatment with PI3K/AKT/mTOR inhibitors have increased infection risk – with the urinary tract being the most likely site of infection.<sup>54</sup> These findings highlight the importance of understanding the role of PI3K/AKT signaling in host defense and evaluating specific PI3K/AKT targets for the development of clinical therapeutics. Ongoing studies in our laboratory are investigating how downstream PI3K/AKT effectors and transcription factors regulate the production of AMPs like RNase 7.

Finally, in this study we demonstrate that increased RNase 7 production protects urothelial cells from UPEC. However, we also show that UPEC strains expressing the pore-forming HlyA toxin have the unique ability to suppress RNase 7. Given our *in vitro* findings, we postulate that HlyA increases UTI risk, recurrence, and severity in part by inhibiting front-line immune defenses like RNase 7. Previously, Wiles *et al* demonstrated that HlyA-expressing UPEC strains inhibit urothelial PI3K/AKT activation via an extracellular calcium-dependent, potassium-independent process that requires HlyA insertion into the host plasma membrane.<sup>37</sup> Although our results suggest that UPEC strains expressing HlyA suppress RNase 7 production via PI3K/AKT inhibition, UPEC cytotoxicity may also contribute to RNase 7 suppression given the mechanisms in which HlyA inhibits PI3K/AKT. At sub-lytic concentrations, HlyA induces urothelial cell apoptosis, alters inflammatory responses, and promotes urothelial exfoliation.<sup>37, 55, 56</sup> In the clinical setting, HlyA-expressing UPEC strains are associated with more severe UTI symptoms and are routinely identified in cases of pyelonephritis and bacteremia.<sup>37</sup> In contrast, only a minority of commensal *E. coli* isolates encode HlyA genes.<sup>57, 58</sup> *In vivo* pyelonephritis models suggest that HlyA enhances UPEC virulence by promoting upper urinary tract colonization, increasing renal parenchymal injury, and amplifying the risk of septicemia.<sup>59</sup> Additional studies are warranted to assess how different UPEC isolates and virulence factors impact RNase 7 production and determine how alterations in RNase 7 production (or other urothelial derived AMPs) effect urothelial injury and UTI severity.

In conclusion, in this study we identify insulin as a PI3K/AKT agonist that induces RNase 7, one of the most potent and abundant AMPs in the human urinary tract. Our results begin to show that insulin-induced RNase 7 has biological relevance in that increased RNase 7 production protects urothelial cells by killing UPEC and minimizing LDH release. Because most of the data presented in this manuscript were generated using *in vitro* models and isolated human specimens, we acknowledge that these same findings may not be recapitulated when confounding variables are introduced *in vivo*. Nevertheless, the results presented here provide a foundation for future studies that may have significant clinical



impact evaluating how the insulin-PI3K/AKT-AMP axis can be utilized to prevent and treat infections in at risk patient populations. If PI3K/AKT signaling defects contribute to infection risk in DM patients, then therapeutic restoration of PI3K/AKT activity may have clinical significance. Thus, we propose that up-regulation of urothelial PI3K/AKT should be considered as a target for future therapeutic modalities in protecting DM patients from UTI. However, we acknowledge that manipulation of the PI3K/AKT pathway may lead to unwarranted side effects. Moreover, the use of RNase 7 for therapeutic purposes does require some degree of caution, as some AMPs are potent biomolecules that can elicit native cell death if applied in high concentrations.<sup>11</sup> Finally, we acknowledge that our results do not definitively demonstrate that insulin-induced RNase 7 protects the host from infection. To date, there is little published evidence showing that induced or suppressed RNase 7 alters infection susceptibility *in vivo*. In part, these studies are limited as RNase 7 expression is restricted to primates. Thus, *in vivo* evaluation of RNase 7's contribution to host defense and the mechanisms that regulate its production is limited.<sup>26, 60</sup> Thus, additional studies and novel models are needed to evaluate the role of PI3K/AKT activity, insulin signaling, and RNase 7 production on host defense *in vivo*.

## Methods

### Patient study approval and human biological specimens

Informed written consent was obtained from all patients participating in this study. For subjects less than 18 years of age, written parental/guardian consent and patient assent were obtained. The Nationwide Children's Hospital (NCH) Institutional Review Board approved this study along with the consent process and documents (IRB 14-00376). Serial urine specimens were collected from patients presenting to the NCH Emergency Department with new-onset T1DM. Before hospital discharge, all patients were started on an insulin regiment of Lantus (glargine)/Novolog (Lispro). Follow-up urine specimens were collected at least 30 days after starting insulin therapy at the NCH diabetes clinic. Control urine samples were obtained from children 1–18 years of age presenting to the NCH Emergency Department or the nephrology clinic. Control patients had no past history of abnormal renal function, structural urinary tract disorders, history of UTI or recurrent infection, or endocrine disorders. They were evaluated in the Emergency Department for non-febrile minor medical complaints.

Human kidney samples were obtained from patients undergoing nephrectomy for renal tumors. Tissue samples were free of microscopic signs of disease or inflammation. Kidney tissue was provided by the Cooperative Human Tissue Network, which is funded by the National Cancer Institute. Other investigators may have received specimens from the same subjects.<sup>13, 61</sup>

### Immunostaining

IHC was performed as previously described.<sup>12</sup> Rabbit polyclonal antibodies were used to label RNase 7 (1:50, Sigma-Aldrich) and IR (1:50, Abcam, Cambridge, MA). Triple label immunofluorescence was performed to localize IR expression in the kidney. All sections were prepared as previously described.<sup>12</sup> Sections were labeled for principal cells with a

goat polyclonal anti-AQP-2 antibody (1:500, Santa Cruz Biotechnology, Santa Cruz, CA, USA) and intercalated cells with a chicken polyclonal anti-V-ATPase E1 subunit antibody (1:2,000, Sigma-Aldrich) or a mouse monoclonal anti-AE1 antibody (1:2,000, kindly provided by M. Jennings).

### Inhibitors and other reagents

Recombinant human insulin and wortmannin were obtained from Sigma-Aldrich (St. Louis, MO). LY204002 was purchased from Cell Signaling Technology (Danvers, MA). AKT inhibitor X was purchased from Cayman Chemicals (Ann Arbor, MI).

### Bacterial strains

*E. coli* strains CFT073, UTI89, and UTI89 *hlyA* were used. UTI89 is a type I-piliated UPEC strain isolated from a patient with cystitis.<sup>62</sup> CFT073 is a UPEC strain isolated from the blood and urine of a patient with pyelonephritis.<sup>63</sup> UTI89 *hlyA* has disruption of the *hlyA* gene (kindly provided by M. Mulvey).<sup>37, 64</sup> *hlyA* gene deletion was verified by polymerase chain reaction (PCR). The hemolytic activity of each UPEC strain was identified and confirmed by growth on blood agar plates at 37°C, where clear zones developed around hemolysin-positive bacterial colonies.

### Cell culture

Primary human mixed renal epithelial cells, originally obtained from a 3-year-old Hispanic female (Lifeline Cell Technology, Frederick, MD), were cultured in RenaLife basal culture medium with supplemental Renalife Lifefactors (Lifeline Cell Technology, Frederick, MD) at 37°C in 5% CO<sub>2</sub>. Primary human urothelial cells, obtained from a 52-year-old white male, were cultured in urothelial cell medium with urothelial growth supplements (Lot#8854, ScienCell Research Laboratories, Carlsbad, CA).<sup>65</sup> Once reaching 80–90% confluency, cells were treated with the indicated drugs or with carrier for the specified times.

5637 human bladder epithelial cells (ATCC HTB-9; American Type Culture Collection, Manassas, VA) were cultured in RPMI 1640 medium (Invitrogen, Carlsbad, CA) supplemented with 10% heat-inactivated fetal bovine serum (HyClone Laboratories, Logan, UT) at 37°C in 5% CO<sub>2</sub>. After reaching confluence, 5637 cells were serum starved overnight. Urothelial monolayers were challenged with UPEC using a multiplicity of infection (MOI) of 25–30 microbes per host cell. Plates were spun at 1,000 rpm for 5 min to expedite and synchronize bacterial contact with the host cell monolayers.<sup>37</sup>

### AKT Transfection

To confirm the influence of AKT on RNase 7 expression, human bladder urothelial cells were transfected with pCMV5-hemagglutinin (HA)-PKB $\alpha$  (wt-AKT), pCMV5-HA-membrane targeted-PKB $\alpha$  (m/p-AKT), or pCMV5-HA-AAHA-PKB $\alpha$  (DN-AKT) (purchased from D. Alessi, University of Dundee, Dundee, United Kingdom). 5637 cells were grown in 24 well plates to 60% confluency. Cells were then transfected with 0.6  $\mu$ g/well of wt-AKT, DN-AKT, or m/p-AKT using Lipofectamine LTX according to the manufacturer's instructions (Invitrogen, Grand Island, NY). Briefly, for each well, 1.2  $\mu$ L of Lipofectamine, 0.6  $\mu$ g plasmid DNA, and 0.5  $\mu$ L Plus Reagent was added to 50  $\mu$ L Opti-

Mem medium (Invitrogen). After 5 min incubation, 50  $\mu$ L was added to each well. 48 hours post-transfection, medias were used for ELISA analysis and protein lysates were isolated for Western blot. Transfection efficiency of approximately 75% was determined via phase and fluorescence microscopy 48 hrs post-transfection with a vector containing an irrelevant protein fused to mCherry (not shown).

### Ex vivo human kidney assay

Human kidney samples were obtained from the Cooperative Human Tissue Network as outlined above. Kidneys from three nephrectomized patients was cut into 150 mg sections and placed in insulin free Renalife basal culture medium with the appropriate inhibitors. Kidneys incubated in medium only served as controls. After a 4-hour incubation at 37°C, the kidneys were homogenized and SDS-Page Western blot was performed.

### RNA isolation and qRT-PCR

Total RNA was isolated from cells using the RNeasy Mini Kit according to the manufacturer's instructions (Qiagen, Hilden, Germany). Up to 2  $\mu$ g of total RNA were reverse transcribed using random hexamer oligonucleotides in a 20 $\mu$ l reaction volume (Verso cDNA Synthesis Kit, Thermo Scientific, Waltham, MA). RNase 7 qRT-PCR was performed as previously described.<sup>12</sup> Specificity of amplification was confirmed by melt-curve analysis and gel electrophoresis. qRT-PCR were analyzed with the threshold cycle method using GAPDH as an internal standard to normalize mRNA amounts. Relative expression changes were calculated using the  $2^{-CT}$  method.<sup>66</sup> Primer sequences used:

*RNASE4* 5' - ATGGCTCTGCAGAGGACCCAT-3' (forward) and

5' -AACCACTCGCGATAATCCCTA-3' (reverse);

*RNASE5* 5' -GCCCGTTTCTGCGGACTTGT-3' (forward) and

5' -ACAACAAAACGCCAGGCC-3' (reverse);

*RNASE7* 5' -AAGACCAAGCGCAAAGCGAC-3' (forward) and

5' -GCAGGCTATTTGGGGTCT-3' (reverse);

*RNASE8* 5' -GGGCCATGTCCCTGACCAT-3' (forward) and

5' -ACCCTGGGTCACCCTGTTGTG-3' (reverse);

*RNASE9* 5' -GCCAGACCACCTACCAAAGAA-3' (forward) and

5' -CCACCCAACGGTGTTTGTAGTA-3' (reverse);

*RNASE12* 5' -GCCAAAACCTTTTCGGCCATT-3' (forward) and

5' -TACCTGCAGGCAGGGTATCT-3' (reverse);

and *GAPDH* 5' -ATGAGCCCCAGCCTTCTCCAT-3' (forward) and

5' -CCAGCCGAGCCACATCGCTC-3' (reverse).

All primers were purchased from Integrated DNA Technology (Iowa City, IA).

### SDS-PAGE Western blot

Western blot was performed as previously described.<sup>21</sup> Primary antibody used included: rabbit anti-RNase 7 (1:1,000; Sigma-Aldrich), rabbit anti-GAPDH (1:5,000; Cell Signaling Technology), rabbit anti-phospho AKT (ser473) (D9E) (1:2,000; Cell Signaling Technology), and rabbit anti-pan AKT (11E7) (1:2,000; Cell Signaling Technology).

### ELISA Assay

Culture media and urinary RNase 7 concentrations were measured via ELISA as previously described.<sup>21</sup> Urinary RNase 7 concentrations were normalized to urine creatinine as measured by ELISA (Oxford Biomedical Research, Rochester Hills, MI).

### UPEC Growth Inhibition Assay

UPEC growth in culture media was evaluated as described.<sup>21</sup> In brief, UPEC (strain CFT073) was cultured in Luria–Bertani broth to an optical density  $OD_{670}=0.07$  (corresponding to  $2 \times 10^8$  CFU/mL) and diluted to  $10^3$  CFU/mL. UPEC ( $2 \mu\text{l}$ ) were added to  $100 \mu\text{l}$  of media in a 96-well flat-bottom plate. When indicated,  $2 \mu\text{l}$  of a polyclonal anti-RNase 7 antibody (Biomatik, Wilmington, DE) was added to each test isolate.<sup>19</sup> Bacterial growth ( $OD_{600}$ ) was monitored using a Synergy HT-multimode microplate reader (BioTek Instruments, Winooski, VT).

### UPEC Colony Count Assay

The bactericidal properties of culture media were evaluated using colony count assays as previously described.<sup>67</sup> Briefly, UPEC (strain CFT073) was cultured as outlined above. UPEC ( $5 \mu\text{l}$ ) was added to  $50 \mu\text{l}$  of media. When indicated,  $1 \mu\text{l}$  of a polyclonal anti-RNase 7 antibody (Biomatik) was added to each test isolate thirty minutes before UPEC inoculation. After 3 hours incubation at  $37^\circ\text{C}$ ,  $10 \mu\text{l}$  of the incubation mixture was plated on LB agar and the number of colony forming units (CFU) was determined the following day.

### LDH Cytotoxicity Assay

HRCs were cultured in RenaLife basal culture medium with supplemental Renalife Lifefactors in 96-well plates. Once reaching 80–90% confluency, HRCs were cultured overnight in insulin-free Renalife media. Next, cells were stimulated with insulin for 24 hours and then challenged with  $10^3$  CFU/mL UPEC (CFT073) for an additional 5 hours. When indicated,  $2 \mu\text{l}$  of a polyclonal anti-RNase 7 antibody (Biomatik) was added 45 minutes prior to UPEC challenge. Per manufacturer's instructions, LDH release into the culture media was measured using the LDH Cytotoxicity Detection Assays (Takara Bio, Kyoto, Japan). HRC cytotoxicity was determined using the following calculation:  $\text{Cytotoxicity (\%)} = [(\text{experimental value} - \text{low control}) / (\text{high control} - \text{low control})] \times 100$ , where culture media served as the low control and HRCs treated with 1% Triton X-100 served as the high control.

### Data Analysis

Data were analyzed using GraphPad Prism 6.0 (GraphPad Software Inc, La Jolla, CA). *Human urine samples*: Continuous variables were evaluated for normal distribution with the

D'Agostino-Pearson omnibus test, with normality defined as a  $p$  value  $> 0.05$ . Comparisons on normally distributed data were performed by unpaired two-tailed t test or by paired t-test when appropriate; otherwise, the nonparametric Mann-Whitney U test (unpaired data) or Wilcoxon signed rank test (paired data) was used. Differences between groups with  $p < 0.05$  were regarded as statistically significant. Correlation studies on normally distributed data were performed using the Pearson correlation analysis, unless otherwise noted. *In vitro studies*: Data from *in vitro* experiments were normally distributed and are presented as means and standard error of mean (SEM). Treated and control cells were compared by one-way ANOVA with Tukey's procedure. Western blot quantitation was performed with Image J software. The relative density of each lane was calculated, normalized to GAPDH, and presented as the adjusted density.<sup>68</sup>

## Supplementary Material

Refer to Web version on PubMed Central for supplementary material.

## Acknowledgments

We would like to acknowledge the Human Cooperative Human Tissue Network for providing the human kidney samples. We would like to thank Jennifer Kline for collecting the human urine specimens and maintaining the urine biorepository.

**Funding:** JDS is supported by the National Institute of Health Grant (NIDDK) K08 DK094970 and the NIDDK Diabetic Complications Consortium Grant DK076169. BB is supported by National Institute of Health Grant (NIDDK) K08 DK102594. SI is supported by National Institute of Health Grant (NIDDK) K08 DK092340. ALS and DH are supported by the National Institute of Health Grant (NIDDK) 1R01 DK106286.

## References

1. Korbel L, Spencer JD. Diabetes mellitus and infection: an evaluation of hospital utilization and management costs in the United States. *J Diabetes Complications*. 2015; 29:192–195. [PubMed: 25488325]
2. Robbins SL, Tucker AW. The Cause of Death In Diabetes -- A Report of 307 Autopsied Cases. *The New England Journal of Medicine*. 1944; 231:865–868.
3. Thakar CV, Christianson A, Himmelfarb J, et al. Acute kidney injury episodes and chronic kidney disease risk in diabetes mellitus. *Clin J Am Soc Nephrol*. 2011; 6:2567–2572. [PubMed: 21903988]
4. Goswami R, Bal CS, Tejaswi S, et al. Prevalence of urinary tract infection and renal scars in patients with diabetes mellitus. *Diabetes Res Clin Pract*. 2001; 53:181–186. [PubMed: 11483234]
5. Shah BR, Hux JE. Quantifying the risk of infectious diseases for people with diabetes. *Diabetes Care*. 2003; 26:510–513. [PubMed: 12547890]
6. Muller LM, Gorter KJ, Hak E, et al. Increased risk of common infections in patients with type 1 and type 2 diabetes mellitus. *Clin Infect Dis*. 2005; 41:281–288. [PubMed: 16007521]
7. Geerlings SE. Urinary tract infections in patients with diabetes mellitus: epidemiology, pathogenesis and treatment. *Int J Antimicrob Agents*. 2008; (31 Suppl 1):S54–57. [PubMed: 18054467]
8. Nicolle LE, Friesen D, Harding GK, et al. Hospitalization for acute pyelonephritis in Manitoba, Canada, during the period from 1989 to 1992; impact of diabetes, pregnancy, and aboriginal origin. *Clin Infect Dis*. 1996; 22:1051–1056. [PubMed: 8783709]
9. Zasloff M. Antimicrobial peptides, innate immunity, and the normally sterile urinary tract. *J Am Soc Nephrol*. 2007; 18:2810–2816. [PubMed: 17942949]
10. Spencer JD, Schwaderer AL, Becknell B, et al. The innate immune response during urinary tract infection and pyelonephritis. *Pediatr Nephrol*. 2014; 29:1139–1149. [PubMed: 23732397]

11. Becknell B, Schwaderer A, Hains DS, et al. Amplifying renal immunity: the role of antimicrobial peptides in pyelonephritis. *Nat Rev Nephrol.* 2015; 11:642–655. [PubMed: 26149835]
12. Spencer JD, Schwaderer AL, Dirosario JD, et al. Ribonuclease 7 is a potent antimicrobial peptide within the human urinary tract. *Kidney Int.* 2011; 80:174–180. [PubMed: 21525852]
13. Spencer JD, Schwaderer AL, Wang H, et al. Ribonuclease 7, an antimicrobial peptide upregulated during infection, contributes to microbial defense of the human urinary tract. *Kidney Int.* 2013; 83:615–625. [PubMed: 23302724]
14. Zasloff M. The antibacterial shield of the human urinary tract. *Kidney Int.* 2013; 83:548–550. [PubMed: 23538695]
15. Becknell B, Spencer JD. A Review of Ribonuclease 7's Structure, Regulation, and Contributions to Host Defense. *Int J Mol Sci.* 2016; 17
16. Torrent M, Sanchez D, Buzon V, et al. Comparison of the membrane interaction mechanism of two antimicrobial RNases: RNase 3/ECP and RNase 7. *Biochim Biophys Acta.* 2009; 1788:1116–1125. [PubMed: 19366593]
17. Torrent M, Badia M, Moussaoui M, et al. Comparison of human RNase 3 and RNase 7 bactericidal action at the Gram-negative and Gram-positive bacterial cell wall. *FEBS J.* 2010; 277:1713–1725. [PubMed: 20180804]
18. Lin YM, Wu SJ, Chang TW, et al. Outer membrane protein I of *Pseudomonas aeruginosa* is a target of cationic antimicrobial peptide/protein. *J Biol Chem.* 2010; 285:8985–8994. [PubMed: 20100832]
19. Wang H, Schwaderer AL, Kline J, et al. Contribution of Structural Domains to the Activity of Ribonuclease 7 against Uropathogenic Bacteria. *Antimicrob Agents Chemother.* 2013; 57:766–774. [PubMed: 23183439]
20. Boix E, Nogues MV. Mammalian antimicrobial proteins and peptides: overview on the RNase A superfamily members involved in innate host defence. *Mol Biosyst.* 2007; 3:317–335. [PubMed: 17460791]
21. Spencer JD, Schwaderer AL, Eichler T, et al. An endogenous ribonuclease inhibitor regulates the antimicrobial activity of ribonuclease 7 in the human urinary tract. *Kidney Int.* 2014; 85:1179–1191. [PubMed: 24107847]
22. Dobrzynski E, Montanari D, Agata J, et al. Adrenomedullin improves cardiac function and prevents renal damage in streptozotocin-induced diabetic rats. *Am J Physiol Endocrinol Metab.* 2002; 283:E1291–1298. [PubMed: 12424108]
23. Kondo T, Kahn CR. Altered insulin signaling in retinal tissue in diabetic states. *J Biol Chem.* 2004; 279:37997–38006. [PubMed: 15201286]
24. Laviola L, Belsanti G, Davalli AM, et al. Effects of streptozocin diabetes and diabetes treatment by islet transplantation on in vivo insulin signaling in rat heart. *Diabetes.* 2001; 50:2709–2720. [PubMed: 11723053]
25. Mariappan MM, Feliars D, Mummidi S, et al. High glucose, high insulin, and their combination rapidly induce laminin-beta1 synthesis by regulation of mRNA translation in renal epithelial cells. *Diabetes.* 2007; 56:476–485. [PubMed: 17259394]
26. Becknell B, Eichler TE, Beceiro S, et al. Ribonucleases 6 and 7 have antimicrobial function in the human and murine urinary tract. *Kidney Int.* 2015; 87:151–161. [PubMed: 25075772]
27. Hale LJ, Coward RJ. Insulin signalling to the kidney in health and disease. *Clin Sci (Lond).* 2013; 124:351–370. [PubMed: 23190266]
28. Butlen D, Vadrot S, Roseau S, et al. Insulin receptors along the rat nephron: [125I] insulin binding in microdissected glomeruli and tubules. *Pflugers Arch.* 1988; 412:604–612. [PubMed: 3211711]
29. Sechi LA, De Carli S, Bartoli E. In situ characterization of renal insulin receptors in the rat. *J Recept Res.* 1994; 14:347–356. [PubMed: 7877134]
30. Bourdeau JE, Chen ER, Carone FA. Insulin uptake in the renal proximal tubule. *Am J Physiol.* 1973; 225:1399–1404. [PubMed: 4760452]
31. Thimmaiah KN, Easton JB, Germain GS, et al. Identification of N10-substituted phenoxazines as potent and specific inhibitors of Akt signaling. *J Biol Chem.* 2005; 280:31924–31935. [PubMed: 16009706]

32. Andjelkovic M, Alessi DR, Meier R, et al. Role of translocation in the activation and function of protein kinase B. *J Biol Chem.* 1997; 272:31515–31524. [PubMed: 9395488]
33. Ganesan LP, Wei G, Pengal RA, et al. The serine/threonine kinase Akt Promotes Fc gamma receptor-mediated phagocytosis in murine macrophages through the activation of p70S6 kinase. *J Biol Chem.* 2004; 279:54416–54425. [PubMed: 15485887]
34. Wang Q, Somwar R, Bilan PJ, et al. Protein kinase B/Akt participates in GLUT4 translocation by insulin in L6 myoblasts. *Mol Cell Biol.* 1999; 19:4008–4018. [PubMed: 10330141]
35. Galluzzi L, Aaronson SA, Abrams J, et al. Guidelines for the use and interpretation of assays for monitoring cell death in higher eukaryotes. *Cell Death Differ.* 2009; 16:1093–1107. [PubMed: 19373242]
36. Seiler F, Hellberg J, Lepper PM, et al. FOXO transcription factors regulate innate immune mechanisms in respiratory epithelial cells. *J Immunol.* 2013; 190:1603–1613. [PubMed: 23315071]
37. Wiles TJ, Dhakal BK, Eto DS, et al. Inactivation of host Akt/protein kinase B signaling by bacterial pore-forming toxins. *Mol Biol Cell.* 2008; 19:1427–1438. [PubMed: 18234841]
38. Brauner H, Luthje P, Grunler J, et al. Markers of innate immune activity in patients with type 1 and type 2 diabetes mellitus and the effect of the anti-oxidant coenzyme Q10 on inflammatory activity. *Clin Exp Immunol.* 2014; 177:478–482. [PubMed: 24593795]
39. Wang H, Li H, Jiang X, et al. Hecidin is directly regulated by insulin and plays an important role in iron overload in streptozotocin-induced diabetic rats. *Diabetes.* 2014; 63:1506–1518. [PubMed: 24379355]
40. Barnea M, Madar Z, Froy O. Glucose and insulin are needed for optimal defensin expression in human cell lines. *Biochem Biophys Res Commun.* 2008; 367:452–456. [PubMed: 18178160]
41. Froy O, Hananel A, Chapnik N, et al. Differential effect of insulin treatment on decreased levels of beta-defensins and Toll-like receptors in diabetic rats. *Mol Immunol.* 2007; 44:796–802. [PubMed: 16740310]
42. Hiratsuka T, Nakazato M, Ihi T, et al. Structural analysis of human beta-defensin-1 and its significance in urinary tract infection. *Nephron.* 2000; 85:34–40. [PubMed: 10773753]
43. Harder J, Schroder JM. RNase 7, a novel innate immune defense antimicrobial protein of healthy human skin. *J Biol Chem.* 2002; 277:46779–46784. [PubMed: 12244054]
44. Page RA, Malik AN. Elevated levels of beta defensin-1 mRNA in diabetic kidneys of GK rats. *Biochem Biophys Res Commun.* 2003; 310:513–521. [PubMed: 14521940]
45. Malik AN, Al-Kafaji G. Glucose regulation of beta-defensin-1 mRNA in human renal cells. *Biochem Biophys Res Commun.* 2007; 353:318–323. [PubMed: 17187760]
46. Zdychova J, Komers R. Emerging role of Akt kinase/protein kinase B signaling in pathophysiology of diabetes and its complications. *Physiol Res.* 2005; 54:1–16. [PubMed: 15717836]
47. Weichhart T, Saemann MD. The PI3K/Akt/mTOR pathway in innate immune cells: emerging therapeutic applications. *Ann Rheum Dis.* 2008; (67 Suppl 3):iii70–74. [PubMed: 19022819]
48. Williams DL, Li C, Ha T, et al. Modulation of the phosphoinositide 3-kinase pathway alters innate resistance to polymicrobial sepsis. *J Immunol.* 2004; 172:449–456. [PubMed: 14688354]
49. Schabbauer G, Tencati M, Pedersen B, et al. PI3K-Akt pathway suppresses coagulation and inflammation in endotoxemic mice. *Arterioscler Thromb Vasc Biol.* 2004; 24:1963–1969. [PubMed: 15319270]
50. Shamri R, Young KM, Weller PF. PI3K, ERK, p38 MAPK and integrins regulate CCR3-mediated secretion of mouse and human eosinophil-associated RNases. *Allergy.* 2013; 68:880–889. [PubMed: 23742707]
51. Kenzel S, Mergen M, von Susskind-Schwendi J, et al. Insulin modulates the inflammatory granulocyte response to streptococci via phosphatidylinositol 3-kinase. *J Immunol.* 2012; 189:4582–4591. [PubMed: 23018458]
52. Brown JB, Cheresh P, Goretzky T, et al. Epithelial phosphatidylinositol-3-kinase signaling is required for beta-catenin activation and host defense against *Citrobacter rodentium* infection. *Infect Immun.* 2011; 79:1863–1872. [PubMed: 21343355]
53. Fukao T, Yamada T, Tanabe M, et al. Selective loss of gastrointestinal mast cells and impaired immunity in PI3K-deficient mice. *Nat Immunol.* 2002; 3:295–304. [PubMed: 11850627]

54. Rafii S, Roda D, Geuna E, et al. Higher Risk of Infections with PI3K-AKT-mTOR Pathway Inhibitors in Patients with Advanced Solid Tumors on Phase I Clinical Trials. *Clin Cancer Res.* 2015; 21:1869–1876. [PubMed: 25649020]
55. Chen M, Jahnukainen T, Bao W, et al. Uropathogenic *Escherichia coli* toxins induce caspase-independent apoptosis in renal proximal tubular cells via ERK signaling. *Am J Nephrol.* 2003; 23:140–151. [PubMed: 12624487]
56. Weinrauch Y, Zychlinsky A. The induction of apoptosis by bacterial pathogens. *Annu Rev Microbiol.* 1999; 53:155–187. [PubMed: 10547689]
57. Johnson JR. Virulence factors in *Escherichia coli* urinary tract infection. *Clin Microbiol Rev.* 1991; 4:80–128. [PubMed: 1672263]
58. Marrs CF, Zhang L, Foxman B. *Escherichia coli* mediated urinary tract infections: are there distinct uropathogenic *E. coli* (UPEC) pathotypes? *FEMS Microbiol Lett.* 2005; 252:183–190. [PubMed: 16165319]
59. O’Hanley P, Lalonde G, Ji G. Alpha-hemolysin contributes to the pathogenicity of piliated digalactoside-binding *Escherichia coli* in the kidney: efficacy of an alpha-hemolysin vaccine in preventing renal injury in the BALB/c mouse model of pyelonephritis. *Infect Immun.* 1991; 59:1153–1161. [PubMed: 1671776]
60. Cho S, Beintema JJ, Zhang J. The ribonuclease A superfamily of mammals and birds: identifying new members and tracing evolutionary histories. *Genomics.* 2005; 85:208–220. [PubMed: 15676279]
61. LiVolsi VA, Clausen KP, Grizzle W, et al. The Cooperative Human Tissue Network. An update. *Cancer.* 1993; 71:1391–1394. [PubMed: 8435815]
62. Mulvey MA, Schilling JD, Hultgren SJ. Establishment of a persistent *Escherichia coli* reservoir during the acute phase of a bladder infection. *Infect Immun.* 2001; 69:4572–4579. [PubMed: 11402001]
63. Mobley HL, Green DM, Trifillis AL, et al. Pyelonephritogenic *Escherichia coli* and killing of cultured human renal proximal tubular epithelial cells: role of hemolysin in some strains. *Infect Immun.* 1990; 58:1281–1289. [PubMed: 2182540]
64. Blomfield IC, McClain MS, Eisenstein BI. Type 1 fimbriae mutants of *Escherichia coli* K12: characterization of recognized afimbriate strains and construction of new fim deletion mutants. *Mol Microbiol.* 1991; 5:1439–1445. [PubMed: 1686292]
65. Lee WY, Savage JR, Zhang J, et al. Prevention of anti-microbial peptide LL-37-induced apoptosis and ATP release in the urinary bladder by a modified glycosaminoglycan. *PLoS One.* 2013; 8:e77854. [PubMed: 24204996]
66. Schmittgen TD, Livak KJ. Analyzing real-time PCR data by the comparative C(T) method. *Nat Protoc.* 2008; 3:1101–1108. [PubMed: 18546601]
67. Diamond G, Yim S, Rigo I, et al. Measuring antimicrobial peptide activity on epithelial surfaces in cell culture. *Methods Mol Biol.* 2010; 618:371–382. [PubMed: 20094876]
68. Gassmann M, Grenacher B, Rohde B, et al. Quantifying Western blots: pitfalls of densitometry. *Electrophoresis.* 2009; 30:1845–1855. [PubMed: 19517440]
69. Deane JA, Fruman DA. Phosphoinositide 3-kinase: diverse roles in immune cell activation. *Annu Rev Immunol.* 2004; 22:563–598. [PubMed: 15032589]



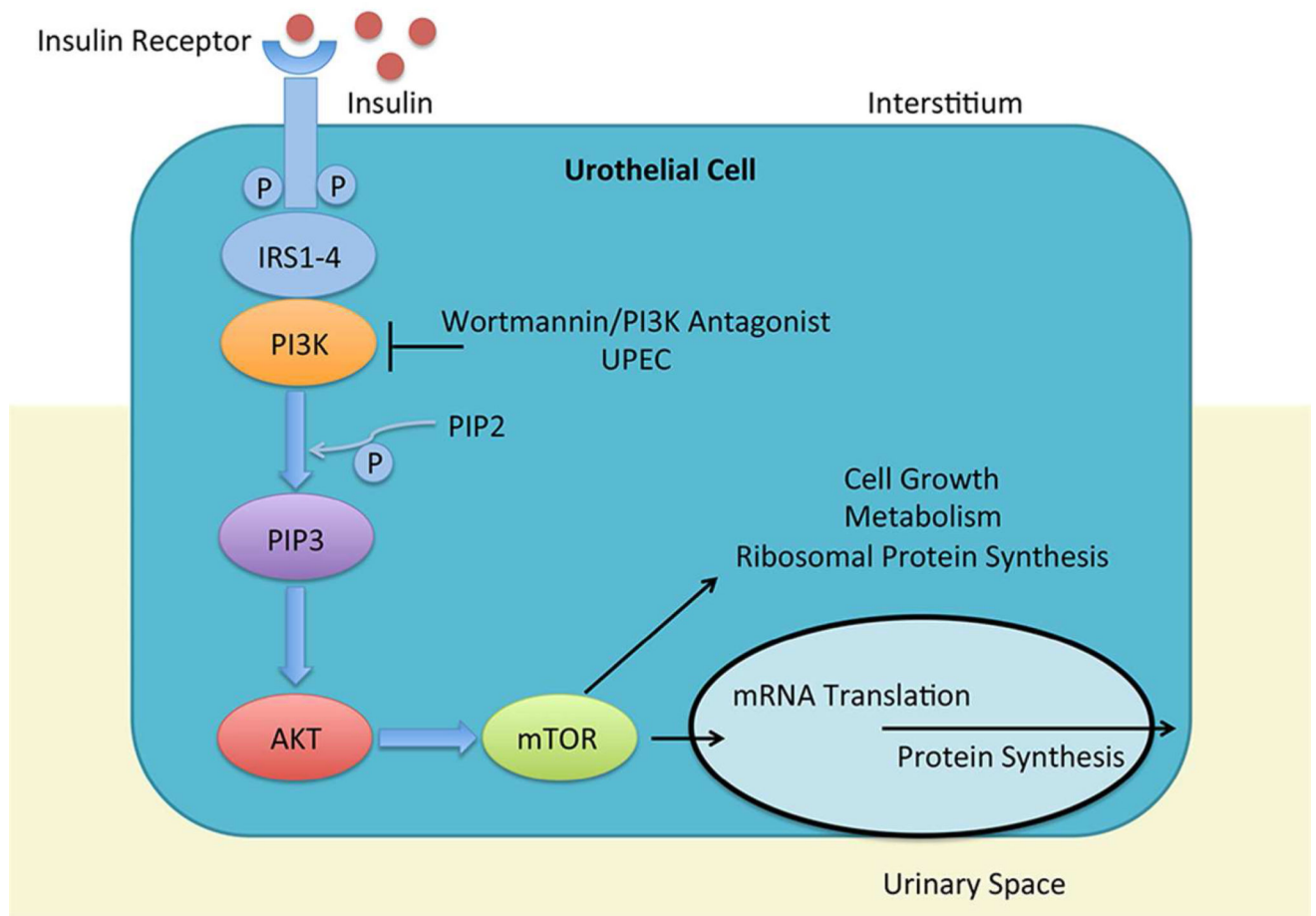


**Figure 1. Insulin and PI3K/AKT signaling**

When insulin enters the bloodstream and binds to its receptor, members of the insulin receptor substrate (IRS) family are activated. IRS, in turn, activates tyrosine kinase adaptor molecules on the cell membrane that recruit class I PI3K to the receptor complex. After receptor engagement, PI3K phosphorylates phosphatidylinositol 4,5 bisphosphate (PIP2) to generate phosphatidylinositol 3,4,5 triphosphate (PIP3) as a second messenger to recruit and activate downstream targets including AKT. AKT, also referred to as Protein Kinase B, is the key downstream effector of PI3K.<sup>69</sup>

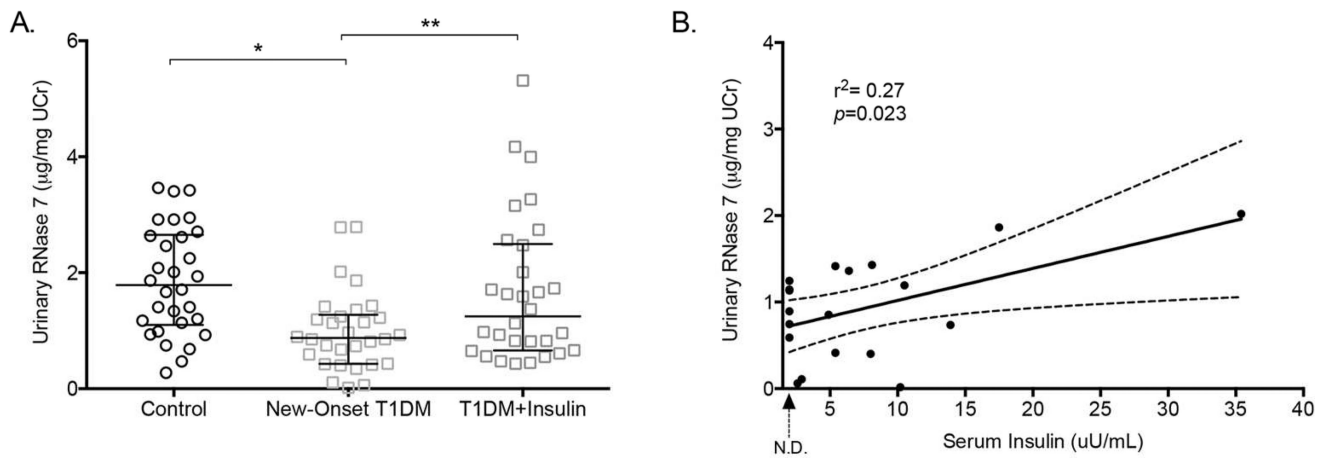


**Figure 2. Insulin increases urinary RNase 7 concentrations in diabetic patients**

(A) Urinary RNase 7 concentrations, standardized to UCr, in control patients ( $n=30$ ) and patients with new-onset type 1 diabetes mellitus ( $n=30$ ) before and after starting insulin therapy. Horizontal bars represent median urinary RNase 7/UCr concentrations and the 25th and 75th percentiles. The symbol \* indicates significant  $p$ -values of less than 0.05, as determined by Mann-Whitney U test. The symbol \*\* indicates significant  $p$ -values of less than 0.05, as determined by the Wilcoxon matched-pairs signed rank test. (B) Pearson correlation analysis demonstrates that urinary RNase 7 concentrations correlate with serum insulin levels in patients with new-onset T1DM. The 95% confidence intervals are represented by the dashed lines ( $n=19$ ). The dashed arrow below the x-axis indicates the lower limit of serum insulin detection (non-detected, N.D.).

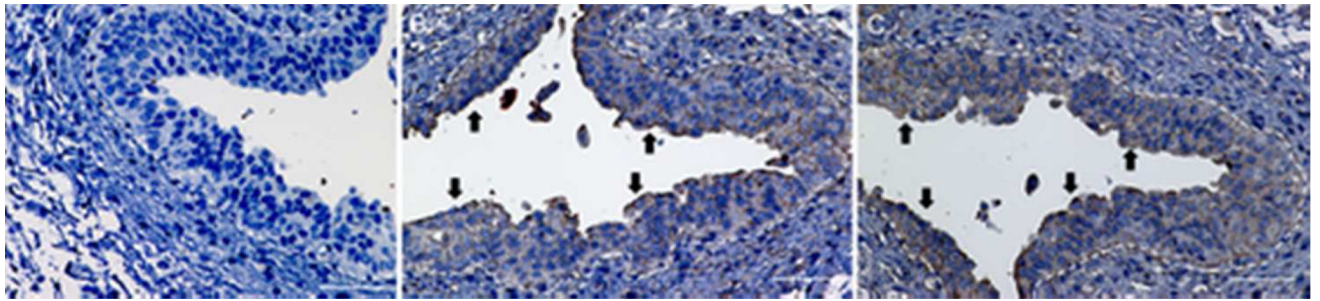


**Figure 3. The human bladder urothelium expresses insulin receptor and RNase 7**  
(A-C) Immunohistochemistry demonstrates (A) negative control, (B) insulin receptor, and (C) RNase 7 production the bladder urothelium (brown, arrows). Dashed lines demarcate the border between the urothelial and stromal layers of the bladder. Magnification 40X. Scale bars represent 200 microns.

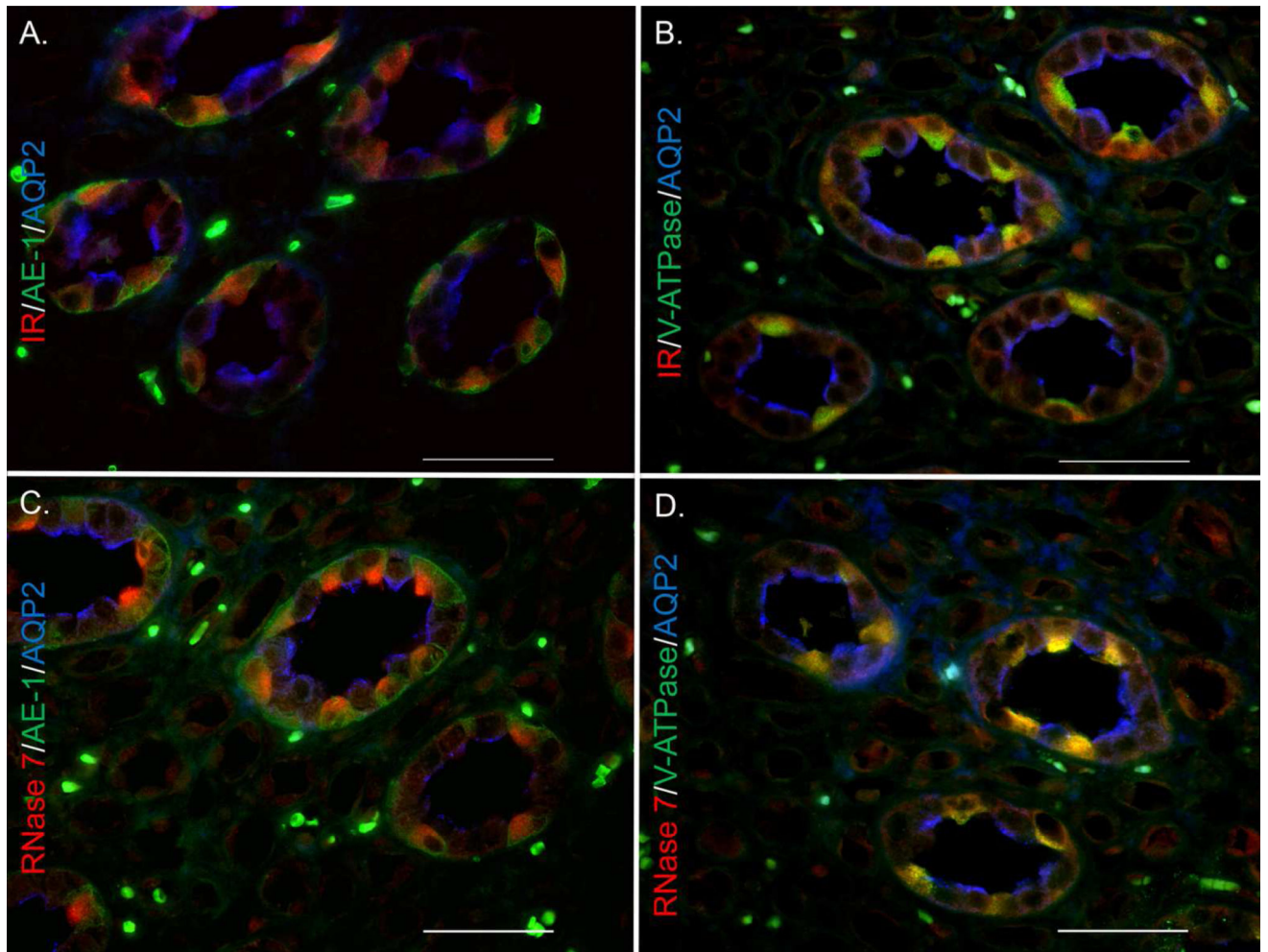


**Figure 4. The kidney collecting tubules express insulin receptor and RNase 7**  
 Human kidney labeled for (A/B) insulin receptor (red), (C/D) RNase 7 (red), and cell specific markers. Cell specific markers consisted of aquaporin-2 (blue) for principal cells and (A/C) AE-1 or (B/D) V-ATPase (green) for intercalated cells. Magnification 60X. Scale bars represent 50 microns.

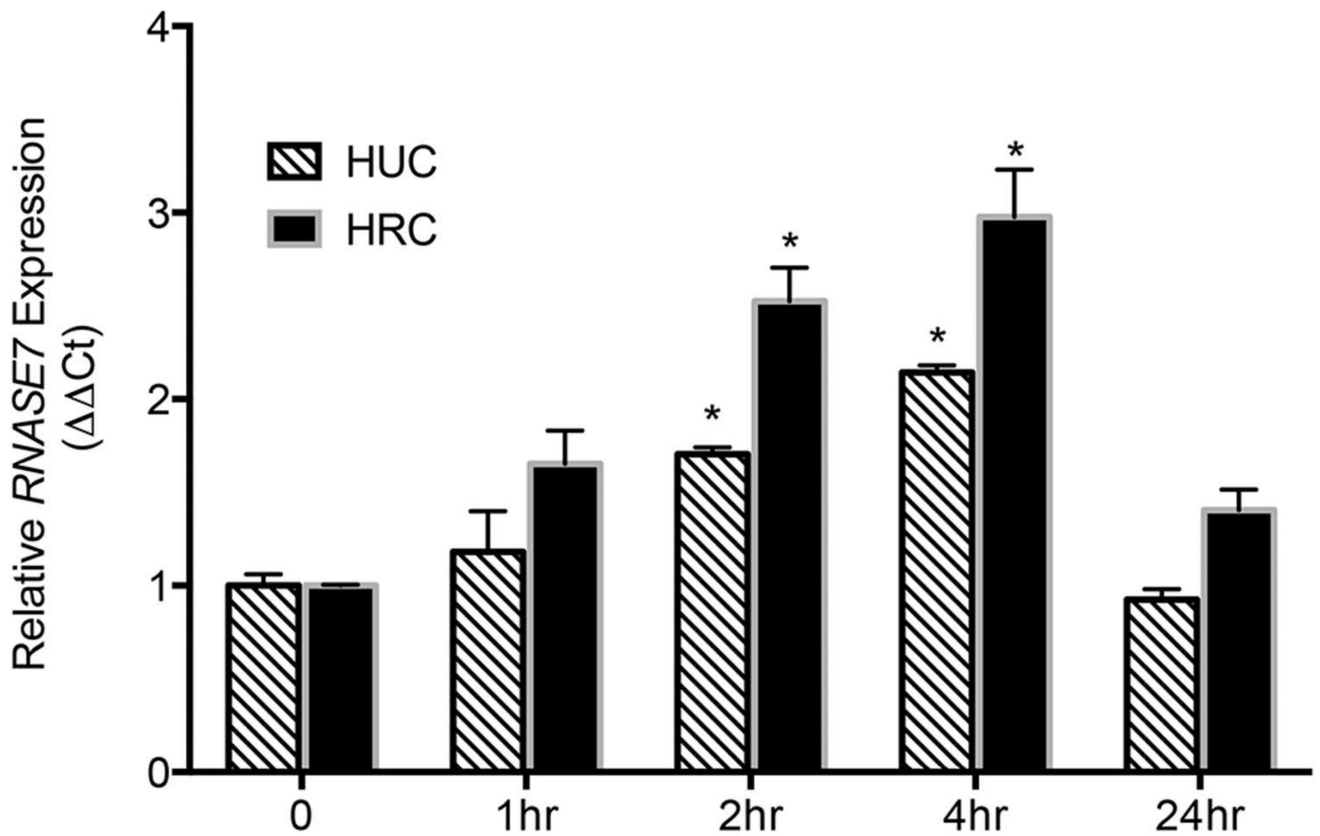


**Figure 5. Insulin induces *RNASE7* mRNA expression over time**

Primary human urothelial cells (HUC) and renal epithelial cells (HRC) were cultured in insulin free media and treated with recombinant human insulin (1 $\mu$ M). Quantitative real-time PCR shows insulin-induced *RNASE7* expression over time. *RNASE7* expression is derived from three independent experiments performed in triplicate ( $n=3$ ). Columns represent means  $\pm$  the standard error of the mean (SEM). The symbol \* indicates significant  $p$ -values of less than 0.05, compared to time zero control for each respective cell type, as determined by one-way ANOVA with Tukey's test.

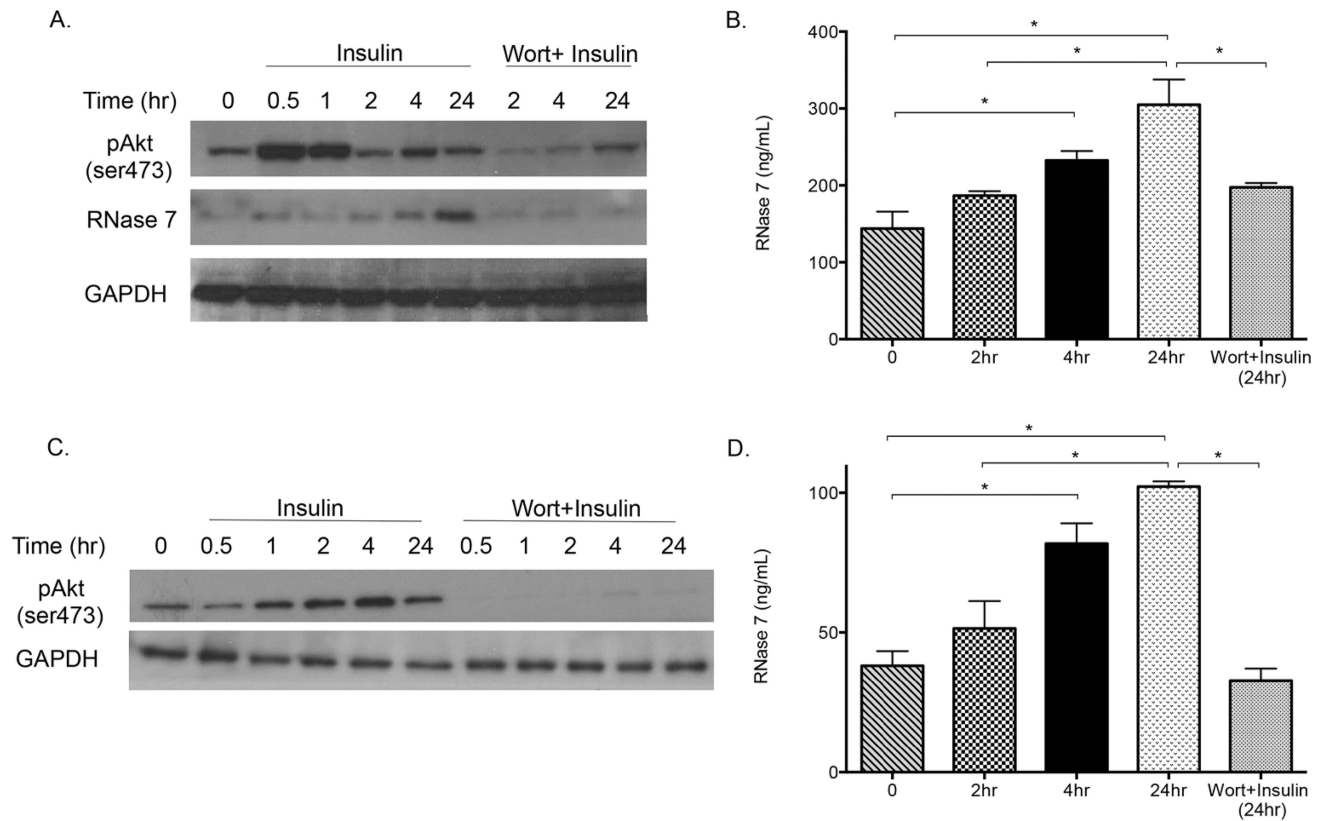


**Figure 6. Insulin induces urothelial PI3K/AKT activity and RNase 7 peptide production**  
 Primary human urothelial cells (HUC) (A/B) and primary human renal epithelial cells (HRC) (C/D) were cultured in insulin free media and stimulated with recombinant human insulin (1 $\mu$ M) for the given time points. Cells were also pretreated with wortmannin (wort, 500 nM) for 1 hour prior to insulin treatment. (A/C) Representative Western blots of HUCs (A) and (C) HRCs probed for pAKT (ser473), RNase 7, and glyceraldehyde 3-phosphate dehydrogenase (GAPDH). RNase 7 was not detected by Western blot in the renal epithelial cells (C). (B/D) ELISA assays quantitated RNase 7 concentration in culture media from (B) HUCs and (D) HRCs following insulin treatment. RNase 7 quantification was derived from three independent experiments performed in triplicate ( $n=4$ ). Columns represent means  $\pm$  SEM. The symbol \* indicates significant  $p$ -values of less than 0.05, for the indicated pairwise comparison, as determined by the one-way ANOVA with Tukey's test.

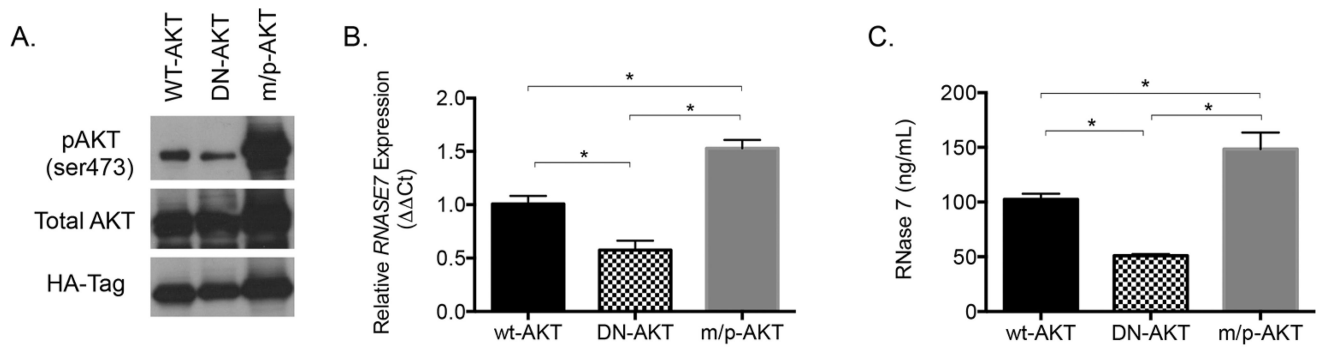


### Figure 7. PI3K/AKT regulates RNase 7 expression

5637 urothelial cells were transfected with plasmids encoding wild-type AKT (wt-AKT), dominant negative AKT (DN-AKT), or membrane targeted AKT (m/p-AKT). (A) Representative Western blots of transfected cell lysates probed to evaluate pAKT (ser473) and total AKT. Anti-HA-Tag antibodies were used to confirm equal transfection efficiency. (B) Quantitative real-time PCR evaluated *RNASE7* mRNA expression in transfected cells. Results are derived from three independent experiments where cells were transfected in quadruplicate ( $n=3$ , columns represent means  $\pm$  SEM). (C) ELISA assays measured RNase 7 concentrations in the transfected cell culture media (columns represent means  $\pm$  SEM). Results are derived from three independent experiments where cells were transfected in quadruplicate ( $n=3$ ). (B/C) The symbol \* indicates significant  $p$ -values of less than 0.05, for the indicated pairwise comparison, as determined by the one-way ANOVA with Tukey's test.

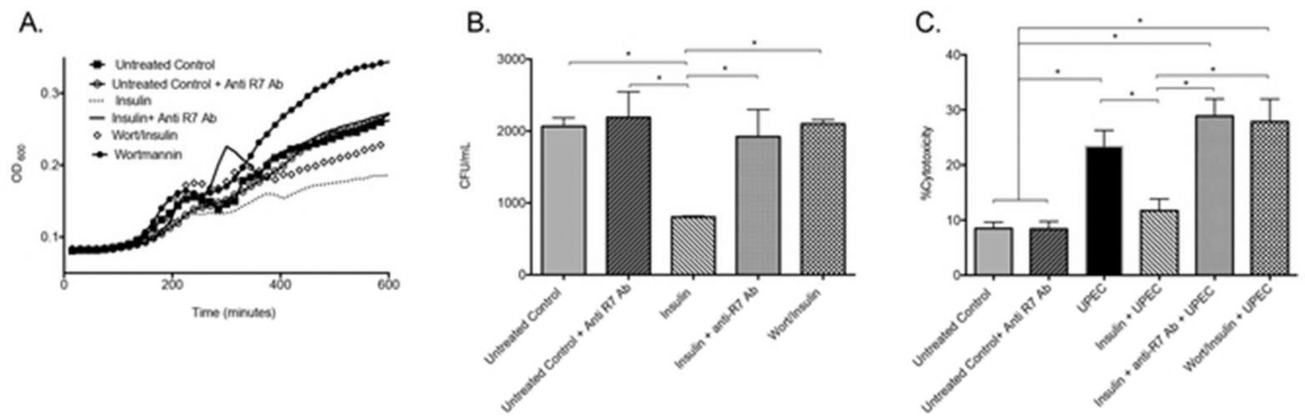


**Figure 8. Insulin-induced RNase 7 suppresses UPEC growth and shields the urothelium from UPEC**

(A) Culture media from untreated control (black squares), 24 hour insulin treated (dashed line), wortmannin+insulin (diamond studded line), or wortmannin treated (black circles) cells were inoculated with *E. coli* (CFT073). UPEC growth was measured by changes in turbidity using the absorbance at 600 nm (OD<sub>600</sub>). Addition of anti-RNase 7 antibody (solid black line) neutralized the antimicrobial activity of RNase 7, resulting in increased bacterial growth. (B) Culture media from untreated control and 24 hour insulin treated were incubated with and without anti-RNase 7 antibody for 30 minutes prior to *E. coli* (CFT073) inoculation. Culture media from wortmannin+insulin treated cells were also inoculated. The number of colony forming units (CFU) was determined after 3 hours incubation. Results are from three independent experiments performed in triplicate ( $n=3$ ). Columns represent means  $\pm$  SEM. The symbol \* indicates significant  $p$ -values of less than 0.05, for the indicated pairwise comparison, as determined by the one-way ANOVA with Tukey's test. (C) Following a 24-hour treatment with insulin (1 $\mu$ M) or wortmannin+insulin, human renal epithelial cells were challenged with UPEC (CFT073). Prior to UPEC challenge, anti-RNase 7 antibody was added to the insulin-stimulated culture media. Five hours after UPEC challenge, LDH release into culture media was measured. Cytotoxicity was calculated as outlined in the Methods section. Results are from six independent experiments performed in quintuplicate ( $n=6$ ). The symbol \* indicates significant  $p$ -values of less than 0.05, for the indicated pairwise comparison, as determined by the one-way ANOVA with Tukey's test.



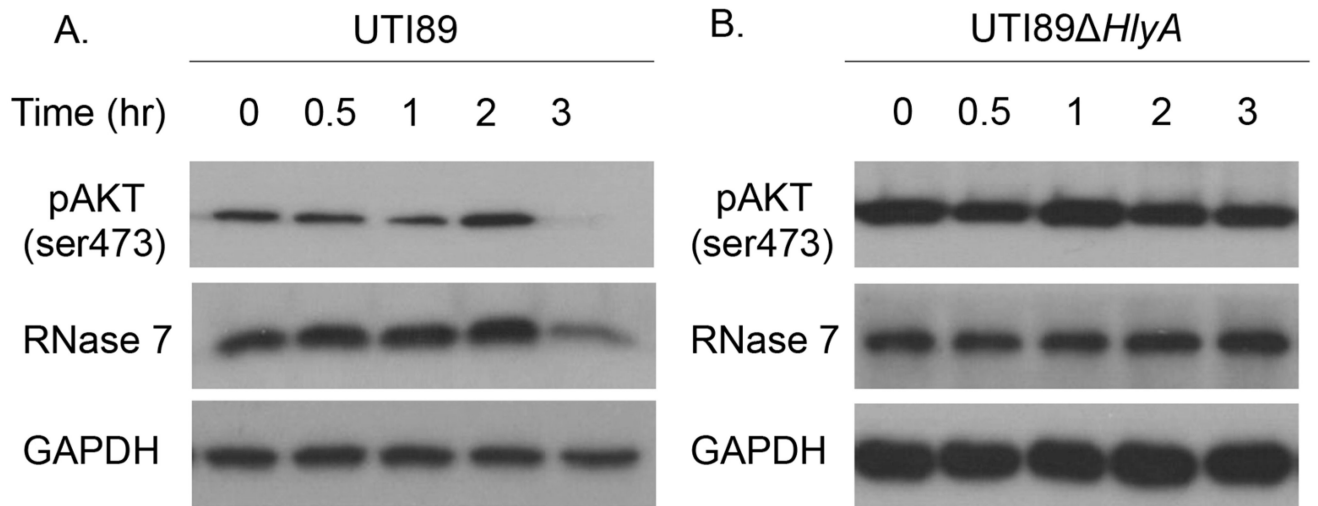


**Figure 9. HlyA-producing UPEC isolates dephosphorylate urothelial AKT to suppress RNase 7**  
Human 5637 urothelial cells were challenged with UPEC strains UTI89 and UTI89 *hlyA* for the indicated times. Shown are representative Western blots of cell lysates probed with antibodies specific for pAKT (ser473), RNase 7, and GAPDH.